

Thiol Diffusion and the Role of Humidity in “Dip Pen Nanolithography”

P. E. Sheehan* and L. J. Whitman

Naval Research Laboratory, Washington, D.C. 20375

(Received 9 November 2001; published 29 March 2002)

The radii of octadecanethiol spots deposited by an atomic force microscope tip onto a gold surface were studied as a function of contact time and humidity. The deposition is well described by two-dimensional diffusion from an annular source of constant concentration, with a surface diffusion coefficient of $8400 \text{ nm}^2 \text{ s}^{-1}$, *independent of humidity*. Facile transfer is observed even after near continuous deposition for more than 24 h in a dry N_2 environment, indicating that a water meniscus is not required.

DOI: 10.1103/PhysRevLett.88.156104

PACS numbers: 68.37.Ps, 68.43.Jk, 81.16.Nd, 81.16.Rf

Since the first use of alkanethiols by Nuzzo and Allara [1] to form a self-assembled monolayer (SAM) on a gold surface, the number of applications for thiolated hydrocarbons has increased rapidly [2], ranging from resists for electronics to biosensor substrates. The major advantages offered by thiol SAMs include long-term stability, versatility in terminal functionality, and ease of use. Perhaps the most attractive feature is their utility for forming small, reproducible surface features outside of a clean room. For example, facile creation of micron-scale patterns has been demonstrated by “stamping” thiols onto a surface using a flexible polymer master, a technique known as microcontact printing (μCP) [3]. Even smaller, nanometer-scale features can be patterned from thiols using the recently developed “Dip Pen Nanolithography” (DPN) [4], where alkanethiols are “written” via transfer from an atomic force microscope (AFM) tip to a surface. The prospect of nanometer-scale control over physical dimensions combined with the flexible terminal group chemistry makes thiol patterning a critical component of many proposed nanotechnologies.

Because alkanethiol patterning is emerging as a key technique for nanofabrication, it is crucial that the mechanisms of deposition—and thereby the ultimate technological potential—be understood. The most important process of the deposition may be diffusion, which controls both the extent and the quality of an alkanethiol SAM. As previously noted in a study of μCP [5], the spatial resolution of a pattern is fundamentally limited by diffusion of the thiol “ink.” First, diffusion of the thiol beyond the initial contact area causes the pattern to be wider than the stamp (for μCP) or the AFM tip terminus (for DPN). Although there have been a few attempts to measure the diffusion rate of thiols on gold [5–8], these measurements have been mostly phenomenological and thus have not reported diffusion coefficients. A second, more subtle, effect of diffusion is its role in the phase transition that occurs during SAM deposition: At a critical surface concentration, the adsorbed thiols reorient from a prone to a standing orientation. This change in orientation affects physical properties of the SAM, such as friction, as well as important chemical properties, such as its ability to mask the substrate from an etchant [9].

Another important issue in determining the overall potential of DPN is the role of water in the deposition process. It is well known that under ambient conditions there is a water meniscus at the AFM tip-surface interface, with a volume that increases with relative humidity (RH) [10]. Beginning with the first reports about DPN [4], it has been suggested that the ink is transported from the tip to the surface through this meniscus. It is unresolved how hydrocarbons, which are essentially insoluble in water, would be transferred in this way, and whether water adsorbed on the surfaces beyond the meniscus affects their transfer and subsequent diffusion. In this Letter, we report the diffusion coefficient for alkanethiol deposition on gold via DPN as a function of humidity. We find that facile deposition occurs for many hours under dry nitrogen, demonstrating that thiol deposition does not occur through the water meniscus.

All experiments were performed using a Nanoscope Multimode AFM (Digital Instruments; Santa Barbara, California) using standard sharpened microlevers. To remove surface contaminants, the tips were soaked in chloroform for 24 h and rinsed with triply distilled H_2O . The rinsed tips were blown dry in filtered N_2 gas and cleaned with ozone for 5 min. AFM tips were coated with octadecanethiol (ODT) by vapor deposition [11] in a glass weighing bottle filled with 100 mg of ODT and heated to 60°C for 30 min. Fresh gold surfaces were prepared from mica-peeled gold [12], which provides reproducible polycrystalline surfaces with a roughness of $\sim 0.2 \text{ nm rms}$. The smoothness of these surfaces minimizes the noise in lateral force microscopy (LFM) images, thereby allowing more precise measurements of ODT island radii as described below.

The radii of octadecanethiol spots deposited by an AFM tip onto a gold surface were measured as a function of tip-surface contact time and relative humidity. Deposition occurred when an ODT-coated AFM tip was lowered into contact with the gold surface allowing the thiol to transfer to the surface and diffuse away. After a set period, the tip was raised and shifted to a new site where it would be left in contact for a longer time. This process was repeated to generate a set of islands created by sequentially longer thiol exposures. (We ensured that the spots were far enough apart to avoid diffusion between them.)

Upon completion of a set, the same tip would be rapidly scanned across the area to form a LFM image at a speed ($>160 \mu\text{m/s}$) sufficient to eliminate significant deposition [4]. A representative image is shown in Fig. 1(a).

During measurements of the diffusion rate, humidity was controlled in one of two ways. To operate in dry nitrogen, a dry bag was placed over the AFM head and scanner and then sealed to the AFM base. Throughout the experiment, filtered N_2 gas was passed through desiccant and into the bag while a high precision digital hydrometer ($\pm 3\%$) in the bag measured the RH. The sample was held in the dry bag for 2 h prior to deposition to minimize water present in the air or on the surfaces. For humidity experiments, a silicone plug (HumPlug, BioForce Laboratory) was used that sealed the sample area of the AFM. To

adjust the humidity, filtered dry nitrogen was mixed with nitrogen that had passed through a glass bubbler containing triply distilled H_2O . For each RH studied, the system was allowed to equilibrate for one hour prior to deposition.

The general process of thiol SAM formation on gold has been described in detail elsewhere [9,13,14]. Briefly, at low concentrations, thiols form a liquid-like phase, where the alkane chains maximize their interaction with the surface by lying prone. When the concentration reaches some critical value, C_s (not generally known), the thiols reorient from this prone position to a more densely packed, standing alignment, as illustrated in Fig. 2(a). As shown in Fig. 2(b), it is possible to image both phases directly with LFM by using a dull tip (radius $>75 \text{ nm}$) and a low contact force. The high-concentration standing phase in the center, appearing as a dark disk, has a relatively low friction coefficient. The surrounding prone region, not as effective at reducing friction, appears as a gray halo. Note that this halo is not apparent when the tip is sharp, presumably because the much greater contact pressure produced by the sharper tip causes it to penetrate through the ODT to the gold surface. The “standing” ODT region has a topographic height of 1.1 nm, lower than that of a fully formed SAM ($\sim 3 \text{ nm}$), indicating that the thiols are standing but not as densely packed [15]. As shown in Fig. 1(b), the radius of the standing region increases smoothly and monotonically with increasing deposition time.

We have developed an approach to extract the diffusion coefficient from such data by modeling the deposition process as follows. The tip is assumed to act as an *infinite reservoir* of molecules, which allows it to maintain a *constant concentration*, C_0 , along the perimeter of the tip-surface contact. Within this assumption, justified by the fact that we can continuously deposit identical features over the time scale of our experiments, all the kinetics of molecular transport from the tip to the surface are included

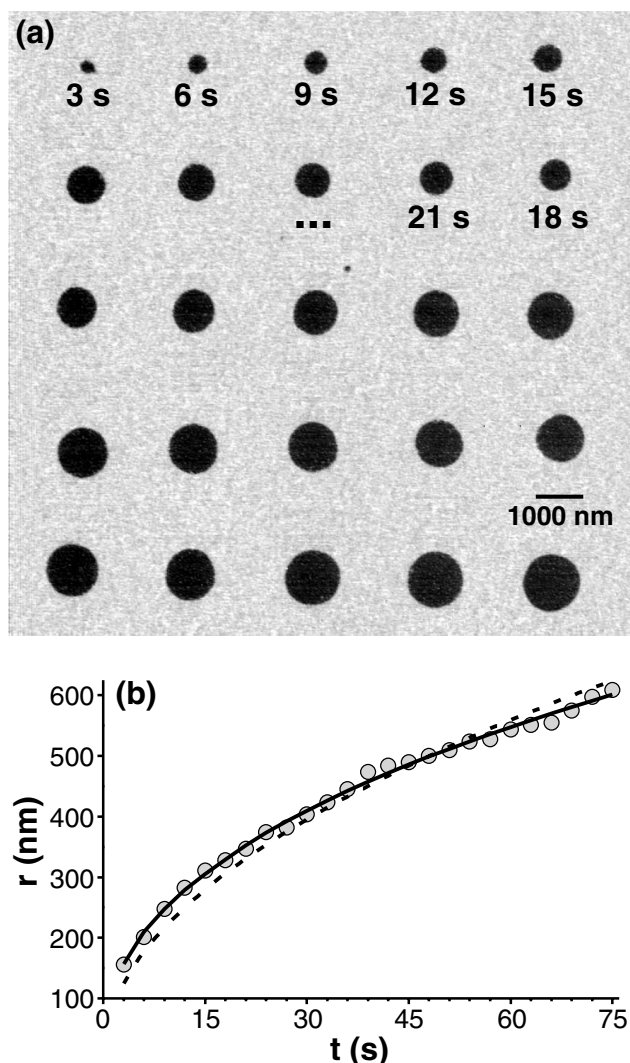


FIG. 1. (a) Friction image of ODT islands deposited on a gold surface by an ODT-coated AFM tip for sequentially longer tip-surface contact. The dark spots are areas of decreased friction caused by the adsorbed ODT. (b) The measured island radii as a function of contact time. The solid line is a fit to the radial diffusion model described in the text. The dashed line is a fit to an alternate model [8] requiring $t^{1/2}$ dependence.

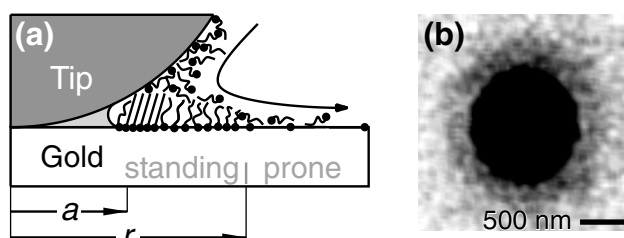


FIG. 2. (a) Scale drawing of the interface between an alkanethiol-coated AFM tip (20-nm radius) and surface. Physisorbed thiols diffuse down the tip to the tip-surface contact area and then diffuse out across the surface, continuously increasing in range and concentration. A SAM of “standing” thiols covers regions of sufficiently high thiol concentration (radius r). The contact radius, a , is defined as the distance at which the tip-surface gap equals the height of the SAM. The light gray area around the tip represents the water meniscus ($\sim 2 \text{ nm}$ high) expected for 60% RH as calculated by the Kelvin equation. (b) Friction image of an ODT island recorded with a dull tip under low load, where both standing (dark) and prone phases (faint halo) can be observed.

in C_0 . Deposited molecules then diffuse radially outward across the substrate. As the island grows outward, the area within the island where the concentration is greater than C_s —and the SAM is standing—expands. Because the thiol-gold binding energy (184 kJ/mol) is comparable to the interaction energy between the alkane backbones (117 kJ/mol) [16], we assume that the diffusion rate across the surface is independent of concentration (“Fickian” diffusion). Finally, when the deposition ends, although some diffusion may continue on the periphery, there is negligible growth of the standing region (as observed experimentally).

Analytically, the surface diffusion is radially symmetric from the tip, with the concentration, c , vanishing at infinite radius, $c(r = \infty) \equiv 0$. For Fickian diffusion, the concentration obeys the two-dimensional diffusion equation [17],

$$\frac{\partial^2 c}{\partial r^2} + \frac{1}{r} \frac{\partial c}{\partial r} = \frac{1}{D} \frac{\partial c}{\partial t}, \quad (1)$$

where r is the radius from the center of the source, t is the time from initial contact, and D is the surface diffusion coefficient. As just described, the tip creates an annular source of radius, a , and constant (but unknown) concentration, $c(r = a) \equiv C_0$ for all t . With these boundary conditions, the diffusion equation can be generally solved using Laplace transforms [18]; however, the exact solution must be numerically integrated and so is not practical for data analysis. Fortunately, an approximate analytical solution has just recently been derived by Smith [19] for cases where r and t are large, which we have identified as being applicable to our physical system. Adapting Smith’s solution yields

$$c(r, t) = C_0 \frac{E_1(r^2/4Dt)}{\ln(4Dt/a^2 e^{2\gamma})}, \quad (2)$$

where E_1 is the exponential integral and γ is Euler’s gamma (≈ 0.577).

Because we measure a series of radii of constant (albeit unknown) thiol concentration, $c(r, t) = C_s$, we can fit our data to this model using only three parameters, C_s/C_0 , a , and D , and thereby determine the surface diffusion coefficient. The contact radius (a) is taken to be the radius at which the tip-surface gap equals the 1.1 nm height of the SAM; i.e., where ODT molecules make contact to both surfaces [see Fig. 2(a)]. This distance can be calculated for each tip based on direct measurement of the tip radius [20], and is comparable to what one would calculate using contact mechanics. The values for C_s/C_0 and D are then found by nonlinear least-squares fitting. Based on 97 series of spot radii vs time taken with numerous AFM cantilevers, the transition concentration C_s/C_0 is 0.12 ± 0.02 . We find the surface diffusion coefficient of ODT deposited on clean gold via DPN to be $8400 \pm 2300 \text{ nm}^2 \text{ s}^{-1}$. As discussed below, this value is independent of humidity.

A number of qualitatively similar experiments have been recently reported [7,21] but analyzed using a different

model [8], where the tip is treated as a source of constant *flux* (as opposed to concentration), and the concentration is zero outside an island. With these assumptions, the island radius should increase as $t^{1/2}$, which is inconsistent with our results [see the dashed line in Fig. 1(b)] [22]. Because the flux is a variable parameter in this alternate model, the absolute diffusion coefficient cannot be determined. We believe our model is more physically realistic, consistent with its more accurate description of our experimental results.

An important question that needs to be addressed is the role of the water meniscus during deposition. Under normal deposition conditions, the meniscus would be quite small. Estimating its size using the Kelvin equation [10], the height of the meniscus even at saturating humidity will be less than the height of a thiol monolayer (Fig. 2), making it unclear how it could serve as an efficient transfer medium. To examine the possible role of water in more detail, we have repeatedly observed the diffusion as a function of humidity in both air and nitrogen. Representative data for three different humidities are displayed in Fig. 3, along with fits to our model. As indicated by the error bars, for each tip, the spot sizes were very reproducible as a function of humidity. Although the RH ranged from 62%, where at least a complete monolayer of water is present on the surface [23], to 0%, where little if any physisorbed water should be present, the diffusion coefficient is essentially unaffected. Although the coefficient increases slightly with decreasing RH in this particular data set, over the course of the ~ 100 experiments performed, no statistically significant dependence on humidity was observed. Significantly, facile deposition occurs *even after many hours in dry nitrogen*.

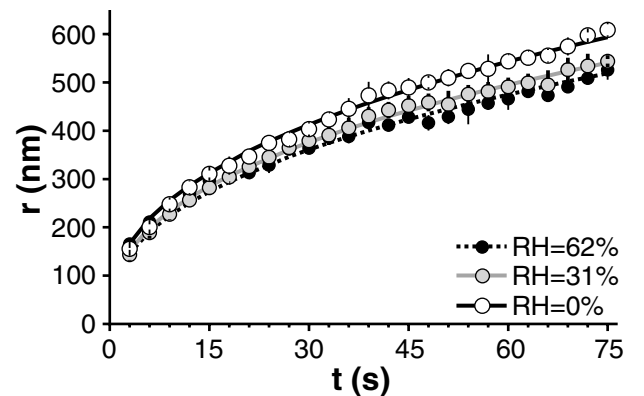


FIG. 3. The radii of ODT islands as a function of deposition time and RH. Each point represents the average radius from four separate deposition sequences, with the error bar showing the standard deviation. The lines represent fits to the model described in the text, which yield diffusion coefficients of 10950, 8664, and 7807 $\text{nm}^2 \text{ s}^{-1}$ for RH of 0%, 31%, and 61%, respectively. Although the coefficient decreases slightly with increasing RH in this data set, over the course of the ~ 100 experiments performed, no statistically significant dependence was observed.

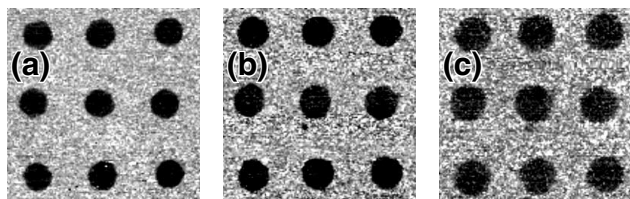


FIG. 4. Images ($7.6 \times 7.6 \mu\text{m}^2$) showing ODT islands deposited sequentially in dry nitrogen (0% RH) from the same tip after (a) 3 h, (b) 12 h, and (c) 26 h. During this sequence, over 1200 islands of ~ 630 nm radius were deposited.

Given these results, the question arises whether water plays any role in the deposition of ODT from an AFM tip to a gold surface. Therefore, the deposition under dry conditions was studied periodically for much longer times in an effort to eliminate remnant physisorbed or weakly chemisorbed water from the surfaces. Significantly, deposition repeatedly continued in dry nitrogen or dry air for over 24 h. Images from one such experiment are shown in Fig. 4, where each island represents a 20-s-long deposition. These experiments clearly demonstrate that a meniscus is not needed for deposition of ODT on gold.

The ability to deposit molecules without a meniscus should be a significant enhancement to the DPN technique. For instance, it should now be possible to use molecules and substrates that are water sensitive or, potentially, to deposit under vacuum. Indeed, given the similarity of our results to those observed for other molecules and substrates [7], these constraints most likely apply to a wide range of systems. The transfer (“on/off”) in these systems will be principally controlled by the chemistry of the ink physisorbed on the tip, whereas the spot size (resolution) will be primarily determined by the diffusion of the ink chemisorbed on the substrate. Furthermore, feature size should be limited to the contact area by modifying the substrate chemistry to decrease the diffusion rate. Ultimately, by reducing the contact area—via carbon nanotube tips, for example—and controlling substrate diffusion, rapid, nanoscale lithography should be achievable by this technique. Moreover, given suitable knowledge of only a few chemical parameters, the process should be quite predictable.

We are indebted to Professor C. A. Mirkin and co-workers for helpful instruction in DPN, and to J. Jang for

insightful discussions. This work was supported by the Air Force Office of Scientific Research and the Office of Naval Research.

*Electronic address: psheehan@stm2.nrl.navy.mil

- [1] R. G. Nuzzo and D. L. Allara, *J. Am. Chem. Soc.* **105**, 4481 (1983).
- [2] A. Ulman, *Chem. Rev.* **96**, 1533 (1996).
- [3] Y. Xia and G. M. Whitesides, *Annu. Rev. Mater. Sci.* **28**, 153 (1998).
- [4] R. D. Piner *et al.*, *Science* **283**, 661 (1999).
- [5] E. Delamarche *et al.*, *J. Phys. Chem. B* **102**, 3324 (1998).
- [6] Y. N. Xia and G. M. Whitesides, *J. Am. Chem. Soc.* **117**, 3274 (1995).
- [7] A. Ivaniseic and C. A. Mirkin, *J. Am. Chem. Soc.* **123**, 7887 (2001).
- [8] J. Y. Jang *et al.*, *J. Chem. Phys.* **115**, 2721 (2001).
- [9] D. K. Schwartz, *Annu. Rev. Phys. Chem.* **52**, 107 (2001).
- [10] A. W. Adamson and A. P. Gast, *Physical Chemistry of Surfaces* (Wiley, New York, 1997).
- [11] S. Hong, J. Zhu, and C. A. Mirkin, *Science* **286**, 523 (1999).
- [12] M. Hegner, P. Wagner, and G. Semenza, *Surf. Sci.* **291**, 39 (1993).
- [13] E. D. Pylant and G. E. Poirier, *Science* **272**, 1145 (1996).
- [14] G. E. Poirier, W. P. Fitts, and J. M. White, *Langmuir* **17**, 1176 (2001).
- [15] K. A. Peterlinz and R. Georgiadis, *Langmuir* **12**, 4731 (1996).
- [16] A. Ulman, *Introduction to Ultrathin Organic Films: From Langmuir-Blodgett to Self-Assembly* (Academic, Boston, 1991).
- [17] J. Crank, *The Mathematics of Diffusion* (Oxford University Press, London, 1975).
- [18] H. S. Carslaw and J. C. Jaeger, *Conduction of Heat in Solids* (Oxford University Press, Oxford, United Kingdom, 1959).
- [19] S. G. L. Smith, *Eur. J. Appl. Math.* **11**, 13 (2000).
- [20] The radius of curvature of each tip was measured after each experiment by imaging very sharp silicon pillars designed for this purpose.
- [21] D. A. Weinberger *et al.*, *Adv. Mater.* **12**, 1600 (2000).
- [22] Unconstrained power law fits to our 97 data sets give an exponent of 0.39 ± 0.06 .
- [23] M. Luna *et al.*, *Appl. Surf. Sci.* **157**, 393 (2000).